

Supplementary Material

Exploring the composition and volatility of secondary organic aerosols in mixed anthropogenic and biogenic precursor systems

Aristeidis Voliotis¹, Yu Wang¹, Yunqi Shao¹, Mao Du¹, Thomas J. Bannan¹, Carl J. Percival², Spyros N. Pandis³, M. Rami Alfarra^{1,4}, and Gordon McFiggans¹

¹Centre for atmospheric science, Department of Earth and Environmental Science, School of Natural Sciences, The University of Manchester, Oxford Road, M13 9PL, Manchester, United Kingdom

²NASA Jet Propulsion Laboratory, California Institute of Technology, 4800 Oak Grove Drive, Pasadena, CA 91109, USA.

³Department of Chemical Engineering, University of Patras, Patras, Greece

⁴National Centre for Atmospheric Science, Department of Earth and Environmental Science, School of Natural Sciences, The University of Manchester, Oxford Road, M13 9PL, Manchester, United Kingdom

Correspondence to: g.mcfiggans.manchester.ac.uk; aristeidis.voliotis@manchester.ac.uk

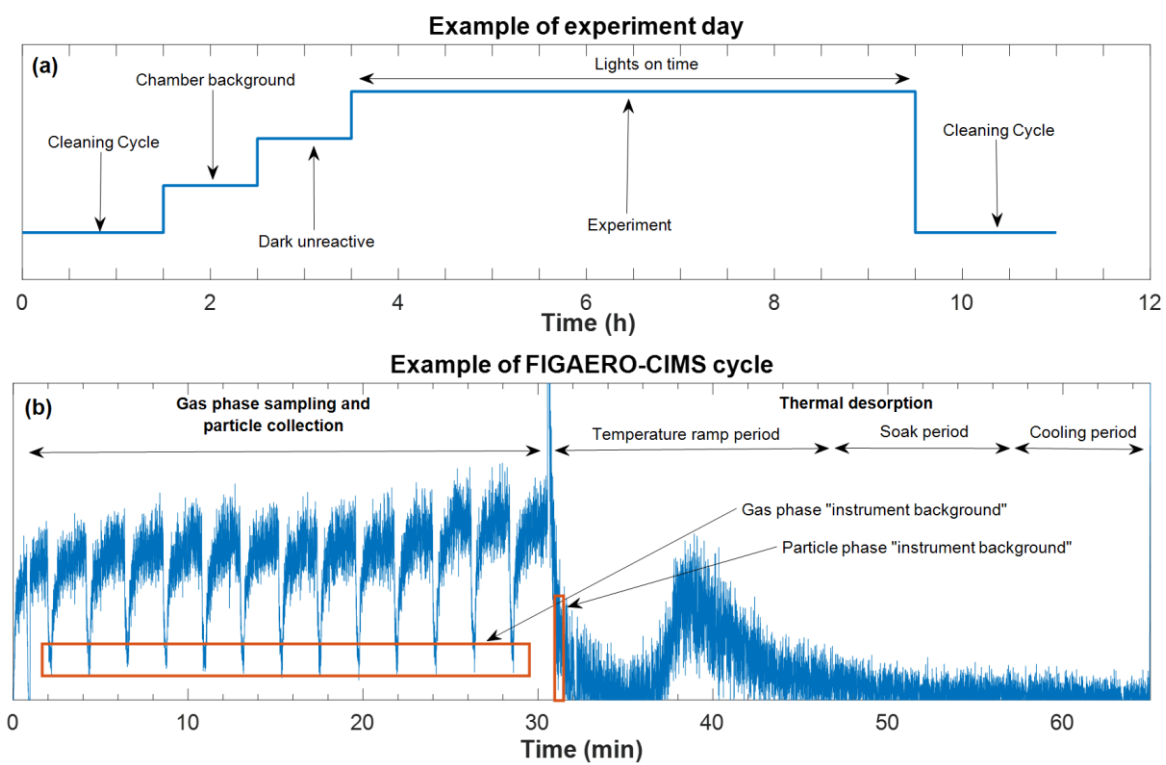


Fig. S1: (a) Schematic of the phases of an experiment, (b) example of FIGAERO-CIMS cycle

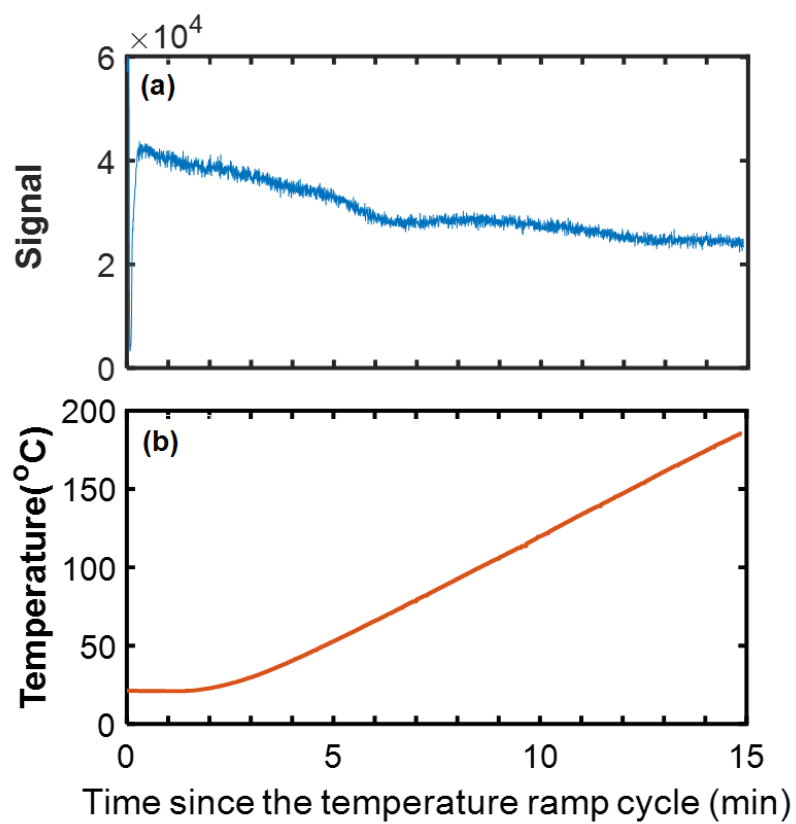


Fig. S2: (a) Example particle phase cycle with contamination from gas phase and (b) example temperature profile of FIGAERO-CIMS during the temperature ramp period.

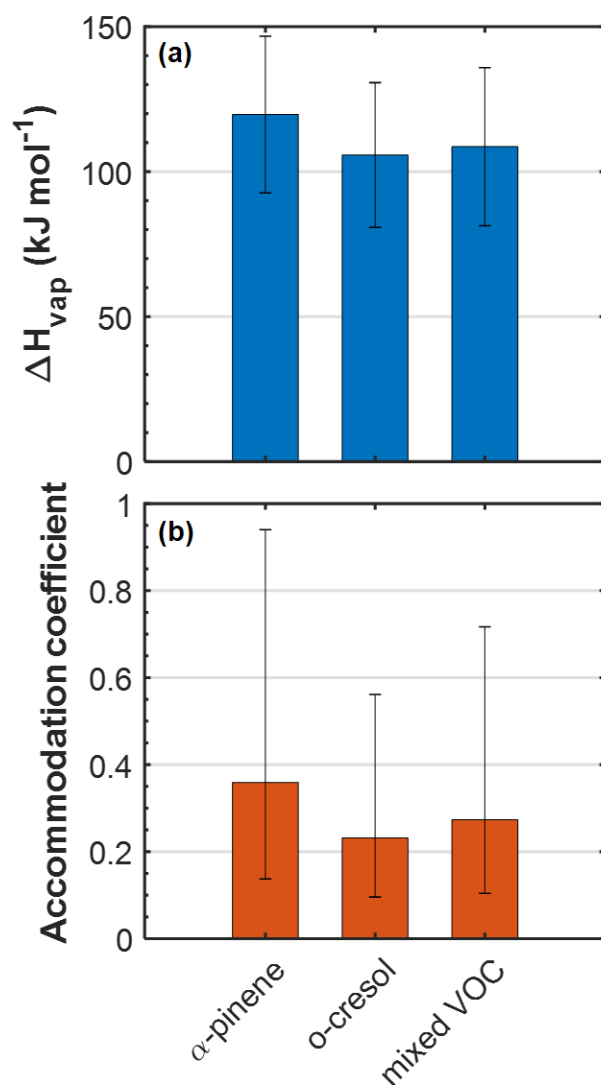


Fig S3: (a) Retrieved enthalpy of vapourisation (kJ mol^{-1}) and (b) accommodation coefficient from the Karnezi et al. (2014) algorithm for three characteristic experiments (Exp. No. 2, 5 and 10; Table 1).

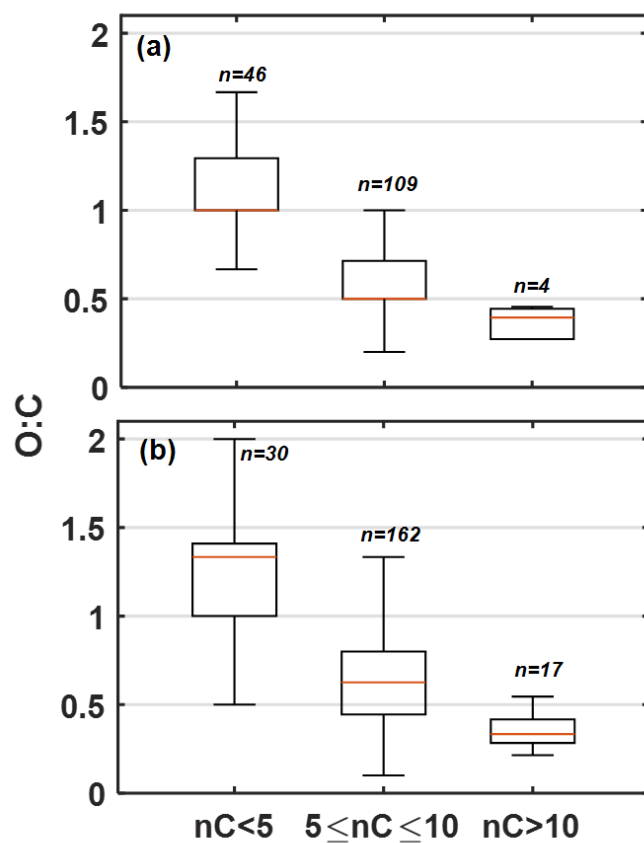


Fig. S4: Boxplots of the O:C ratio of (a) the bulk products found in the mixed VOC system (i.e., unique products of α -pinene, *o*-cresol and common) and (b) products that were found unique in the mixed VOC system, weighted to their contribution to the total signal. Red lines represent the median values, each boxes' upper and lower limits represent the 75th and 25th percentile, respectively, while the errorbars represent the minimum and maximum values.

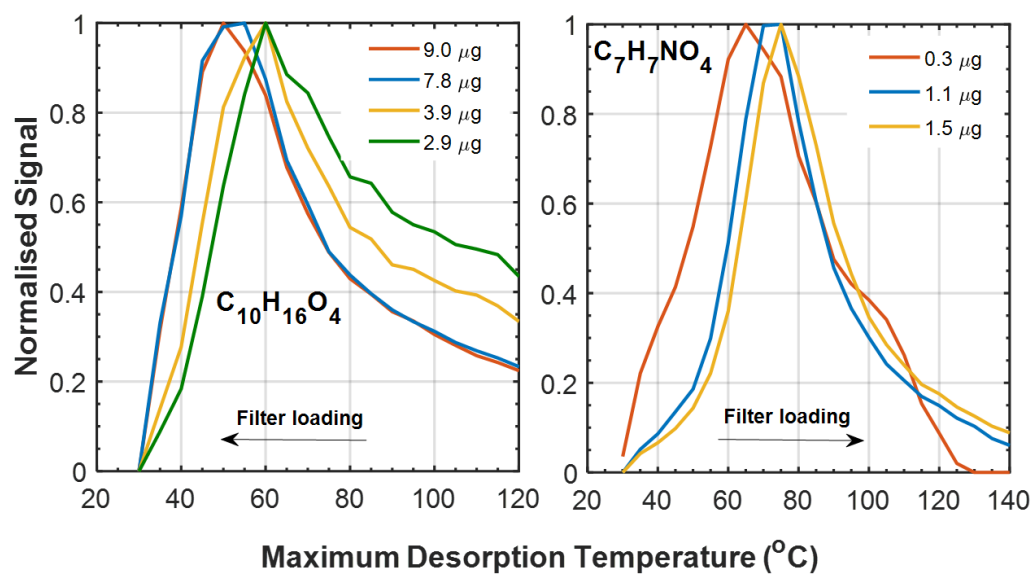


Fig. S5: Thermograms of two characteristic products found at the α -pinene (left panel) and o-cresol and mixed VOC (right panel) systems, at different filter loadings.

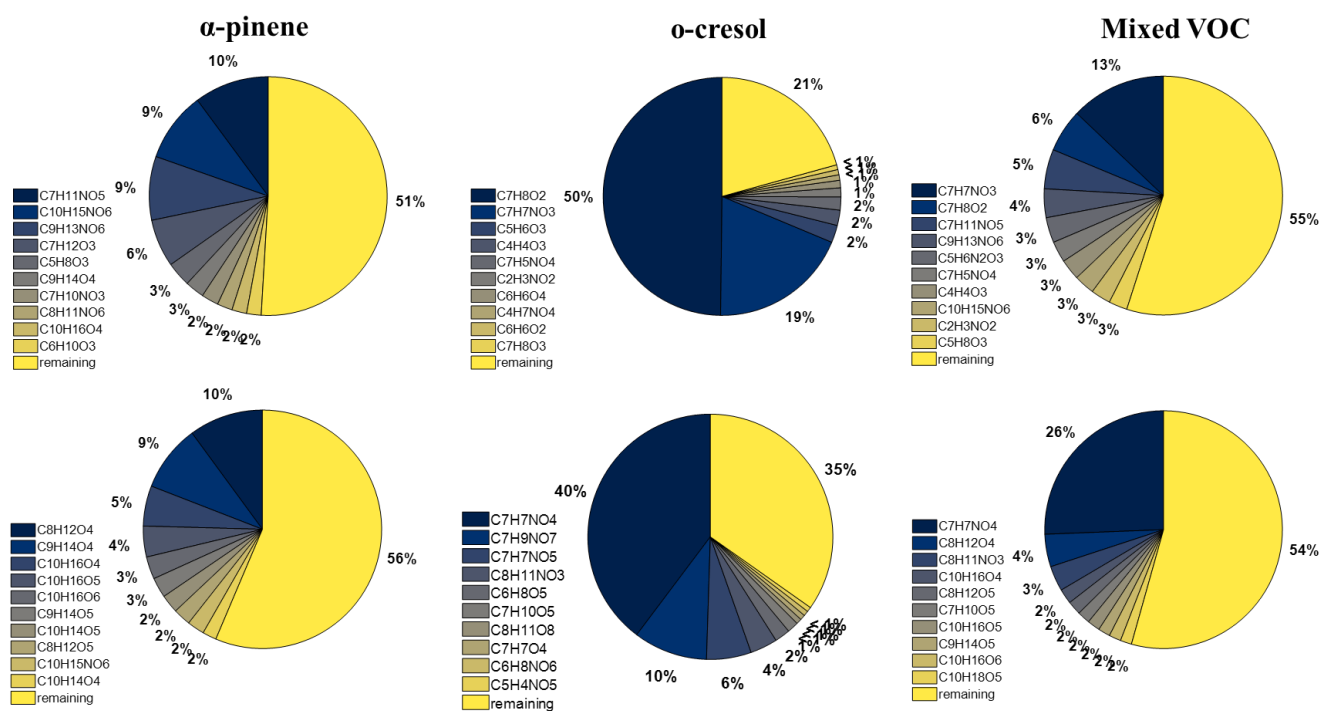


Fig. S6: FIGAERO-CIMS top 10 formula contributions to total signal of three characteristic experiments (Exp. no. 2, 5 and 10; Table 1) for the gas (top charts) and particle (bottom charts) phases.

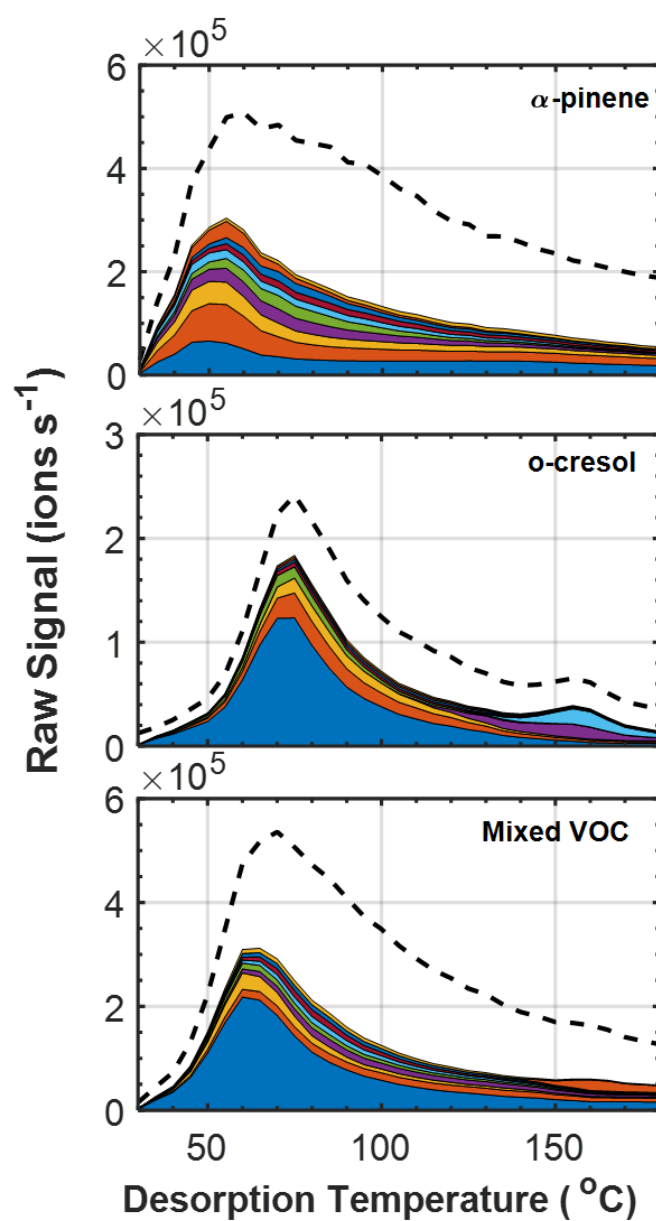


Fig. S7: FIGAERO-CIMS sum thermograms (dashed lines) and top 10 products areas (Fig. S6) for three characteristic experiments in each system (Exp. No. 2, 5 and 10; Table 1).

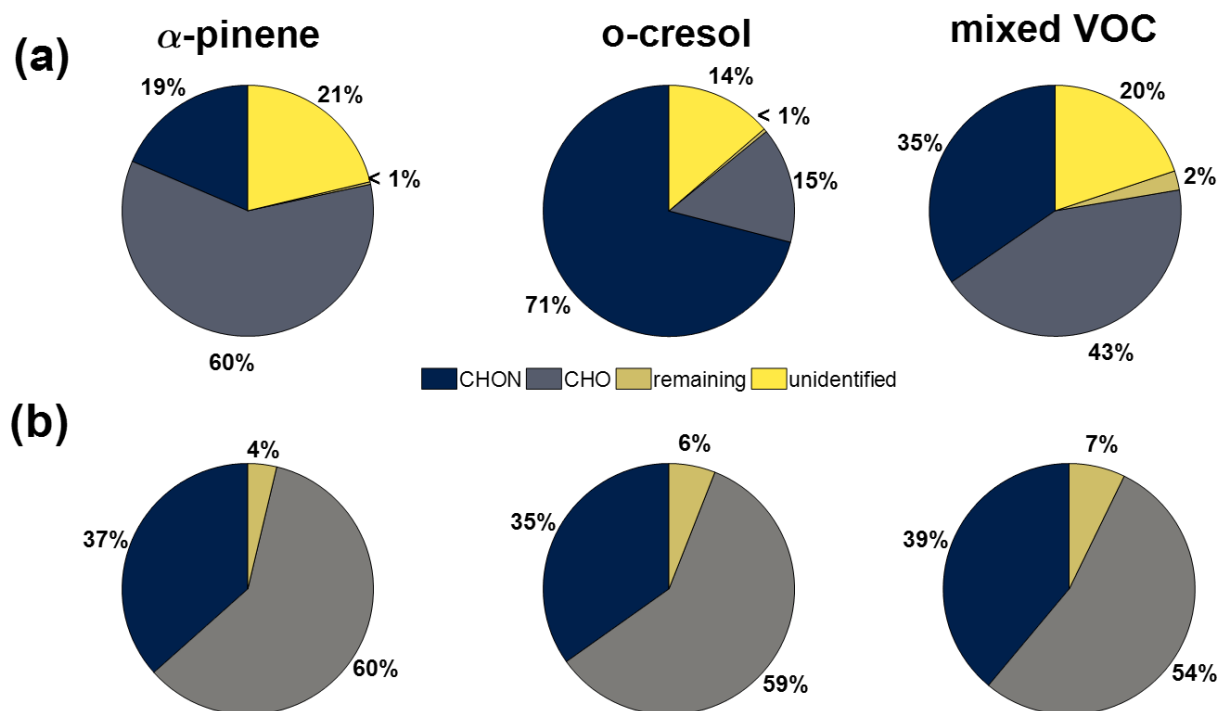


Fig. S8: Particle phase FIGAERO-CIMS elemental formula (a) signal contributions and (b) number fraction of products identified, in three characteristic experiments for each system (Exp. No. 2, 5 and 10; Table 1).

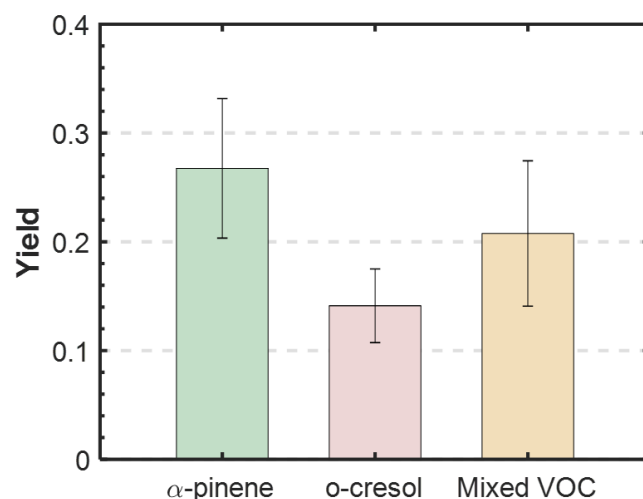


Fig. S9: SOA particle yields (\pm measurement error) obtained in each system. The SOA yields were estimated as the mass of SOA particles formed for each unit mass ($\mu\text{g m}^{-3}$) of VOC consumed (i.e., $Y = \Delta M / \Delta \text{VOC}$). The SOA particle mass formed was obtained from the AMS and the resulted mass was corrected for particle losses to the chamber walls based on the decay rate of ammonium sulfate particles in experiments conducted in the dark. The mass of VOC consumed were obtained from the FIGAERO-CIMS and the GC-MS for the *o*-cresol and α -pinene, respectively. The VOC consumed was computed based on the decay of the raw signal and the initial VOC amounts injected to chamber. All the reported SOA particle yields here were calculated at the maximum SOA particle mass in each experiment.